

Spin label electron paramagnetic resonance study in thylakoid membranes from a new herbicide-resistant D1 mutant from soybean cell cultures deficient in fatty acid desaturation

I. Yruela ^{a,*}, M. Alfonso ^a, I. García-Rubio ^b, J.I. Martínez ^b, R. Picorel ^a, P.J. Alonso ^b

^a Estación Experimental de Aula Dei, Consejo Superior de Investigaciones Científicas, Apdo 202, E-50080 Zaragoza, Spain

^b Instituto de Ciencia de Materiales de Aragón, Consejo Superior de Investigaciones Científicas Universidad de Zaragoza, Plaza S. Francisco s/n, E-50009 Zaragoza, Spain

Received 22 May 2001; received in revised form 25 July 2001; accepted 31 July 2001

Abstract

The effect of fatty acid desaturation on lipid fluidity in thylakoid membranes isolated from the STR7 mutant was investigated by electron paramagnetic resonance (EPR) using spin label probes. The spectra of both 5- and 16-*n*-doxylstearic acid probes were measured as a function of the temperature between 10 and 305 K and compared to those of the wild type. This complete thermal evolution provides a wider picture of the dynamics. The spectra of the 5-*n*-doxylstearic acid probe as well as their temperature evolution were identical in both STR7 mutant and wild type thylakoids. However, differences were found with the 16-*n*-doxylstearic acid probe at temperatures between 230 and 305 K. The differences in the thermal evolution of the EPR spectra can be interpreted as a 5–10 K shift toward higher temperatures of the probe motional rates in the STR7 mutant as compared with that in the wild type. At temperatures below 230 K no differences were observed. The results indicated that the lipid motion in the outermost region of the thylakoids is the same in the STR7 mutant as in the wild type while the fluidity in the inner region of the STR7 mutant membrane decreases. Our data point out a picture of the STR7 thylakoid membrane in which the lipid motion is slower most probably as a consequence of fatty acid desaturation deficiency. © 2001 Elsevier Science B.V. All rights reserved.

Keywords: Electron paramagnetic resonance spectroscopy; Fatty acid saturation; Lipid fluidity; Spin label; Thylakoid

Abbreviations: *A*, hyperfine constant, hyperfine tensor; BSA, bovine serum albumin; Chl, chlorophyll; D1, protein encoded by the *psbA* gene of the photosystem II reaction centre; ΔB_{pp} , peak to peak linewidth; DGDG, digalactosyldiacylglycerol; EPR, electron paramagnetic resonance; *g*, giromagnetic factor, giromagnetic tensor; MES, 2-(*N*-morpholino)ethanesulphonic acid; MGDG, monogalactosyldiacylglycerol; NO[•], doxyl(4,4-dimethyl-*N*-oxy-2-oxazolidinyl); PG, phosphatidylglycerol; PS, photosystem; SASL, stearic acid spin label; SQDG, sulphoquinovosyldiacylglycerol; STR7, atrazine-resistant D1 mutant from *Glycine max*; τ_c , correlation time; $\nu_{\mu w}$, microwave frequency; WT, wild type

* Corresponding author. Fax: +34-976-71-61-45.

E-mail address: yruela@ead.csic.es (I. Yruela).

1. Introduction

The thylakoid membrane of higher plant chloroplasts is highly specialised to assembly protein and pigment molecules, which drive the efficient absorption of light and its conversion into chemical energy. It consists of extensive planar lamellae bound by tightly curved margins and enclosing an inner aqueous compartment, the lumen. This network of membranes can be divided into appressed (grana), non-appressed (stroma) and marginal regions. Its functional constituents are organised into four major supramolecular protein complexes: photosystem (PS) I, PS II, cytochrome *b₆f* and ATP synthase complexes. Electron transport in thylakoid membranes is achieved through a spatial organisation of chlorophyll–protein complexes linked together by protein and non-protein redox components. These constituents are characterised by an asymmetric distribution in both the lateral and transversal planes of the thylakoid membrane, thus conferring vectorial properties to the membrane (for reviews see [1–3]). All the membrane components are embedded in a lipid matrix with a characteristic lipid composition that differs from that of biological membranes of non-plant origin. Instead of phospholipids, the major lipids in the thylakoid membrane are glycolipids, which account for approx. 80% of total acyl lipids. Thylakoid membranes of higher plant chloroplasts contain four major lipid classes: monogalactosyldiacylglycerol (MGDG), digalactosyldiacylglycerol (DGDG), sulphoquinovosyldiacylglycerol (SQDG) and phosphatidylglycerol (PG). The lipid molecules are esterified with highly unsaturated fatty acids [4].

Alterations in chloroplast lipids and their metabolism have been observed as effect of a large number of environmental factors affecting plants. In particular, changes in lipids have been noted for plants grown at different temperatures. A generally observed phenomenon is that fatty acid unsaturation increases following low temperature stress and opposite alterations accompany high temperature treatments [5,6]. These changes are consistent with functional requirements for bulk membrane lipids in terms of fluidity to stabilise the structural arrangement and via lipid–protein interactions in integrating the protein complexes and maintaining their spatial distribution. Therefore, lipids in biological mem-

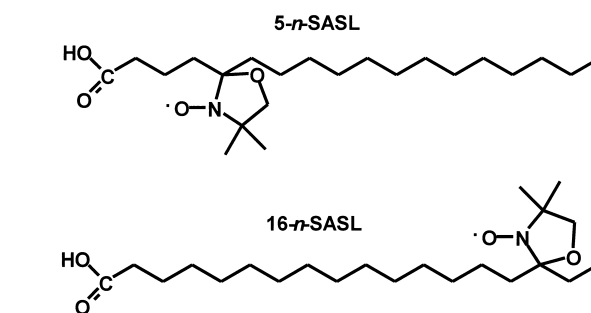


Fig. 1. Formulae of the paramagnetic probes used in our study: 5-*n*-SASL, 5-*n*-doxylstearic acid; 16-*n*-SASL, 16-*n*-doxylstearic acid.

branes play an important role in their physiological function [6–8].

Previously, we reported the characterisation of a new atrazine-resistant mutant (STR7) isolated from photosynthetic cell suspension cultures of soybean with a single new mutation in the chloroplastic *psbA* gene (S268P substitution) [9]. STR7 belongs to a new class of atrazine-resistant mutants affected in the redox couples involving Q_A and Q_B . It presents an unusual tolerance to high temperatures that contrasts with the higher sensitivity to heat stress reported as a feature linked to the triazine resistance trait. The thylakoid membrane of the STR7 mutant accumulates a high content of saturated fatty acids [10]. Therefore, it would be interesting to study whether modifications in the membrane composition cause changes in its fluidity.

The fluidity of biological membranes is a complex phenomenon that has been investigated by spectroscopic methods. Fluorescence or electron paramagnetic resonance (EPR) studies for the analysis of the mobility of fluorescent or spin probes, respectively, inserted into the lipid bilayer have been reported [11–16]. Numerous works have used the EPR signal of nitroxyl (NO \cdot) probes mainly to get information about fluidity and lipid–protein interaction, because the hyperfine interaction anisotropy of the nitroxide is in the order of the characteristic frequencies of some motions in the lipid membranes. The present situation of this subject is reviewed in [17–20]. Those studies were limited to a very reduced temperature region near room temperature. In the present work, we have investigated by EPR the lipid mobility in the thylakoid membrane of two photosynthetic cell lines,

wild type (WT) and STR7, of soybean that differ in lipid composition and fatty acid unsaturation degree, the polypeptide composition being unchanged. To this aim, we used the fatty acid nitroxide probes 5- and 16-*n*-doxylstearic acids (Fig. 1). A wider temperature evolution (from 10 K to 305 K) is presented in order to get a picture as complete as possible of the dynamical processes.

2. Materials and methods

2.1. Biological material

Photosynthetic cell suspension cultures from the higher plant soybean (*Glycine max* var. Corsoy) WT and STR7 mutant were grown in KN1 medium as previously described by Alfonso et al. [9]. Both cell suspensions were cultured at 25°C under continuous light ($75 \mu\text{mol m}^{-2} \text{s}^{-1}$) on a rotatory shaker at 130 rpm in a 5% CO₂ atmosphere.

2.2. Isolation of thylakoid membranes

Cells from 3-week-old cultures were harvested by filtration through a layer of Miracloth paper (Boehringer), resuspended in 400 mM NaCl, 5 mM MgCl₂, 0.2% (w/v) bovine serum albumin (BSA) and 20 mM Tricine (pH 8.0), and disrupted during 10 min with a Teflon homogeniser. To avoid heating, the cell suspensions were kept on ice and the homogenisation process was stopped for 2 min every 2 min. The resulting cell extract was gently stirred for 10 min at 4°C to promote the release of chloroplasts retained within the cell debris. The extract was centrifuged at $300 \times g$ for 1 min and the supernatant centrifuged again at $13\,000 \times g$ for 10 min. The sediment (chloroplasts) was resuspended in 150 mM NaCl, 5 mM MgCl₂ and 20 mM Tricine, pH 8.0 and centrifuged again at $10\,000 \times g$ for 10 min. The sediment (thylakoids) was resuspended in buffer containing 300 mM sucrose, 15 mM NaCl, 5 mM MgCl₂ and 50 mM 2-(*N*-morpholino)ethanesulphonic acid (MES)-NaOH (pH 6.0) and kept at 4°C until use. Under these conditions, the activity of wild type thylakoids was $240 \mu\text{mol O}_2 (\text{mg Chl})^{-1} \text{h}^{-1}$ using 2,6-dichlorobenzoquinone (DCBQ) as the electron acceptor.

2.3. Spin labelling of thylakoid membranes

Thylakoid membranes were resuspended at 1 mg Chl ml⁻¹ in 1 ml buffer containing 15 mM NaCl, 5 mM MgCl₂ and 50 mM MES-NaOH (pH 6.0) and added to a tube containing a film of 5-*n*-doxylstearic (5-*n*-SASL) or 16-*n*-doxylstearic (16-*n*-SASL) acid spin probe (Sigma). The spin label film was prepared on the bottom of an Eppendorf tube by drying 20 μl of a 1 mM *n*-SASL in chloroform. The sample was vortexed briefly, stopping for 1 min every 0.5 min, and incubated for 30 min in the dark at 4°C. The spin-labelled sample was centrifuged at $10\,000 \times g$ for 10 min and twice washed with 15 mM NaCl, 5 mM MgCl₂ and 50 mM MES-NaOH (pH 6.0) [21]. The pellet from the final centrifugation was resuspended at 1 mg Chl ml⁻¹ and transferred to the EPR quartz tube sample holder. A spin probe to lipid ratio below 1:100 (w/w) was used and no spin–spin interactions were detected at this ratio.

2.4. EPR measurements

EPR measurements were carried out in an ESP380E Bruker spectrometer working in X-band. A dielectric high Q-factor (model ER4118dlq) or a high sensitivity (model ER4108tmh) cavity was used. Samples were introduced into 1 mm inner diameter quartz tubes in order to minimise dielectric loss. This is important especially at temperatures higher than 0°C since the samples are aqueous solutions. A Bruker ERV4111T variable temperature system cooled with liquid nitrogen (temperatures higher than 100 K) and the Oxford Inst. CF935 cryostat refrigerated with liquid helium (at lower temperatures) were used.

3. Results

The thermal evolutions of the EPR spectra of the two SASL probes are noticeably different. Thus, we present the corresponding results separately.

3.1. 5-*n*-SASL probe

The EPR spectra of the 5-*n*-SASL probe as well as their temperature evolution are identical in both WT

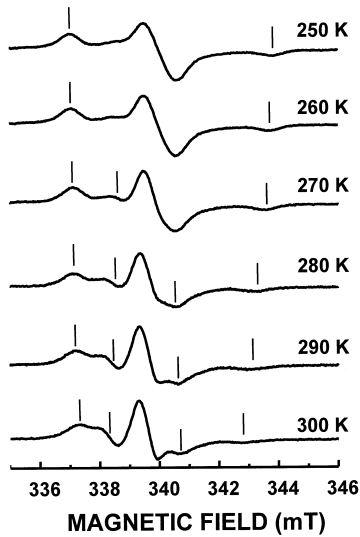


Fig. 2. EPR spectrum of the 5-*n*-SASL probe in STR7 thylakoid membranes at different temperatures.

and STR7 thylakoid membranes. In Fig. 2 we present the spectra measured in the STR7 membrane at different temperatures between 250 and 300 K.

At 250 K, the spectrum corresponds to an axial $S = 1/2$ entity with a hyperfine (*hf*) interaction with a $I = 1$ nucleus (^{14}N). No differences are found when the spectrum is measured below this temperature down to 10 K (data not shown). This signal can be described using the following spin-Hamiltonian:

$$H = \mu_B B \{g_{\perp} (I_x S_x + I_y S_y) + g_{\parallel} I_z S_z\} +$$

$$A_{\perp} (I_x S_x + I_y S_y) + A_{\parallel} I_z S_z \quad (1)$$

where μ_B is the Bohr magneton, g_{\parallel} and g_{\perp} the principal values of the axial g -tensor, B is the DC magnetic field and I_x , I_y , I_z are the director cosines between the field direction and the principal axes of the g -tensor. By fitting the calculated spectrum using the former spin-Hamiltonian to the observed one the following values are obtained:

$$g_{\parallel} = 2.005 \quad g_{\perp} = 2.010 \quad A_{\parallel} = 95 \text{ MHz} \quad A_{\perp} \leq 20 \text{ MHz}$$

At higher temperatures, between 250 and 300 K, changes in the spectrum are observed (Fig. 2). Both STR7 and WT membranes present a similar behaviour: as the temperature increases, the distance between the outermost signals decreases and two new signals appear in the intermediate field that tend to

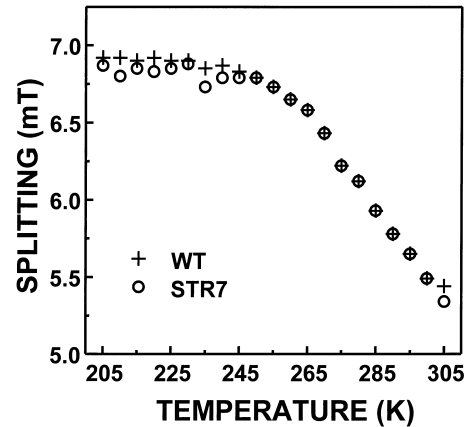


Fig. 3. Splitting between the outermost lines of the 5-*n*-SASL spectrum as a function of temperature. +, WT thylakoid membrane; O, STR7 thylakoid membrane.

collapse with the external ones. This behaviour is illustrated in Fig. 3 where the separation between the external lines is represented as a function of the temperature in both STR7 and WT membranes.

3.2. 16-*n*-SASL probe

The temperature evolution of the 16-*n*-SASL spectrum shows three stages in both the STR7 mutant and the WT thylakoid membranes. The 16-*n*-SASL spectrum in the mutant membrane measured at different temperatures is shown in Fig. 4. At the lowest

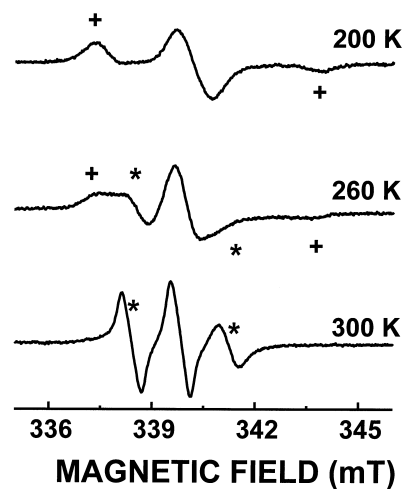


Fig. 4. EPR spectrum of the 16-*n*-SASL probe in the STR7 thylakoid membrane at different temperatures. +, contribution of the axial spectrum (low temperature, 200 K); *, contribution of the isotropic averaged spectrum (high temperature, 300 K).

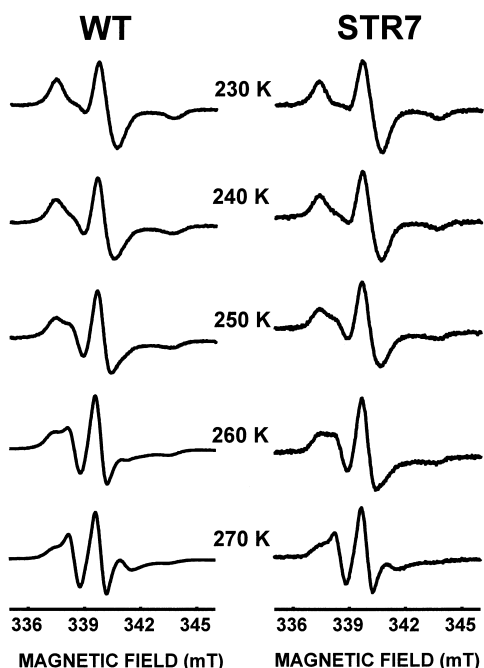


Fig. 5. Detailed thermal evolution of the 16-*n*-SASL spectrum in the transition region. (Left) WT thylakoid membrane; (right) STR7 thylakoid membrane.

temperatures, between 10 and 200 K, the spectrum is very similar to that of the 5-*n*-SASL probe (see 250 K trace in Fig. 2). It can also be described with the same spin-Hamiltonian given in Eq. 1 with practically the same values for the parameters (hereafter called *axial* signal). On the other hand, at temperatures higher than 280 K the spectrum corresponds to an $S = 1/2$ entity interacting with an $I = 1$ nucleus (^{14}N) in the fast motion limit, as the modulation of the different *hf* components indicates (*isotropic* signal). For instance, see the spectrum at 300 K in Fig. 4. A gyromagnetic factor $g = 2.009$ and a *hf* interaction constant $A = 41.5$ MHz are obtained in this case. At intermediate temperatures the spectrum is a superposition of both the *axial* and the *isotropic* signals, and the proportion between them seems to change as a function of temperature.

At low temperature, the spectra of 16-*n*-SASL in both WT and STR7 thylakoid membranes coincide. However, differences are detected at intermediate and high temperatures. The detailed temperature evolution of these spectra in the temperature range between 230 K and 270 K is shown in Fig. 5. The spectra measured in the STR7 membrane are similar to those observed in the WT one at slightly lower

temperatures (about 5–10 K). It is worth mentioning that differential scanning calorimetry (DSC) experiments indicated that the phase transition temperature of the STR7 thylakoid membrane is 5 K higher than that of the WT [10].

Assuming an isotropic reorientation process it is possible to estimate, for the *isotropic* signal, the motion correlation time, τ_c , from the relative intensity of the *hf* components following the procedure outlined in [11]. Taking into account that the intensities of the *hf* components, y_m , are inversely proportional to their half-width squares and considering the alternating line width theory [22] together with the relationship between the half-width and the peak to peak distance, it follows that:

$$\tau_c = \frac{1}{\nu_{\mu\text{w}}} \frac{15\hbar\mu_B}{28\pi} \frac{g^2}{(\tilde{g}' : \tilde{A}')} \frac{\sqrt{3}}{2} \Delta B_{\text{pp}} \left\{ \sqrt{\frac{y_0}{y_{+1}}} - \sqrt{\frac{y_0}{y_{-1}}} \right\} = k \Delta B_{\text{pp}} \left\{ \sqrt{\frac{y_0}{y_{+1}}} - \sqrt{\frac{y_0}{y_{-1}}} \right\} \quad (2)$$

where $\nu_{\mu\text{w}}$ is the microwave frequency, g the isotropic g -factor, ΔB_{pp} the peak to peak distance of the central line (in magnetic field units) and $(\tilde{g}' : \tilde{A}')$ is given by:

$$(\tilde{g}' : \tilde{A}') = \frac{2}{3}(g_{\parallel} - g_{\perp})(A_{\parallel} - A_{\perp}) \quad (3)$$

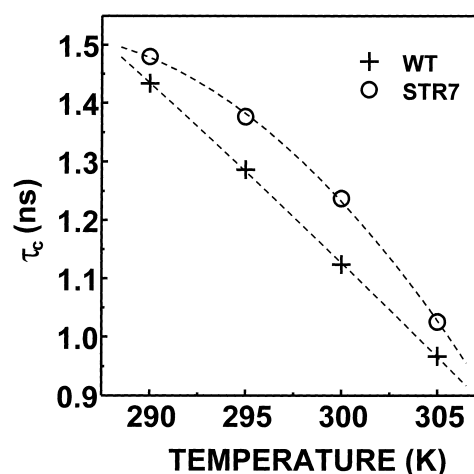


Fig. 6. Temperature evolution of the estimated correlation time, τ_c , (see text) for the reorientation of the isotropic signal in the 16-*n*-SASL spectrum. +, WT thylakoid membrane; O, STR7 thylakoid membrane. Lines are eye-guides.

Using the values for the spin-Hamiltonian parameters quoted above we obtain for our experiments a value of $k=3.4$ when the peak to peak distance, ΔB_{pp} , is expressed in mT and the correlation time, τ_c , in ns. The values for τ_c estimated in this way from the high temperature spectra of 16-*n*-SASL in both WT and STR7 membranes are plotted in Fig. 6. In spite of the crudeness of the model and the small available temperature region as a consequence of the interferences of the *axial* signal, these data point to higher values of the correlation times in the STR7 mutant membrane than in the WT one.

Concerning the *axial* signal the overall splitting slightly decreases as the temperature rises but a complete evolution cannot be followed because of its broadening. In any case, it indicates that it is in a slow motion regime at these low temperatures.

4. Discussion

Changes in the lipid fluidity in thylakoid membranes from two photosynthetic cell lines (STR7 and WT) with different degrees of fatty acid unsaturation were investigated by following the thermal evolution of the EPR spectra of SASLs incorporated into the membranes. The thermal evolution between about 200 and 300 K of the EPR spectra described above clearly indicates the existence of dynamical processes that induce motion of the paramagnetic probes, with a characteristic frequency comparable to the anisotropy of the signal. In order to analyse these results with the aim of getting information about the dynamical properties of the STR7 mutant thylakoid membrane as compared with that of the WT it is necessary to consider the structure of the membranes as well as that of the used probes.

The membranes are constituted by lipids forming a bilayer structure, with the proteins incorporated inside. A schematic model of the membrane is displayed in Fig. 7a. It is worth mentioning that whereas the lipid bilayers form different lyotropic liquid crystal phases, the presence of proteins in biological membranes favours more ordered structures. At low temperatures the membrane is in a L_β gel phase characterised by a rigid disposition of the lipid in the bilayer. As the temperature rises the membrane reaches the liquid crystalline L_α phase. This is mainly

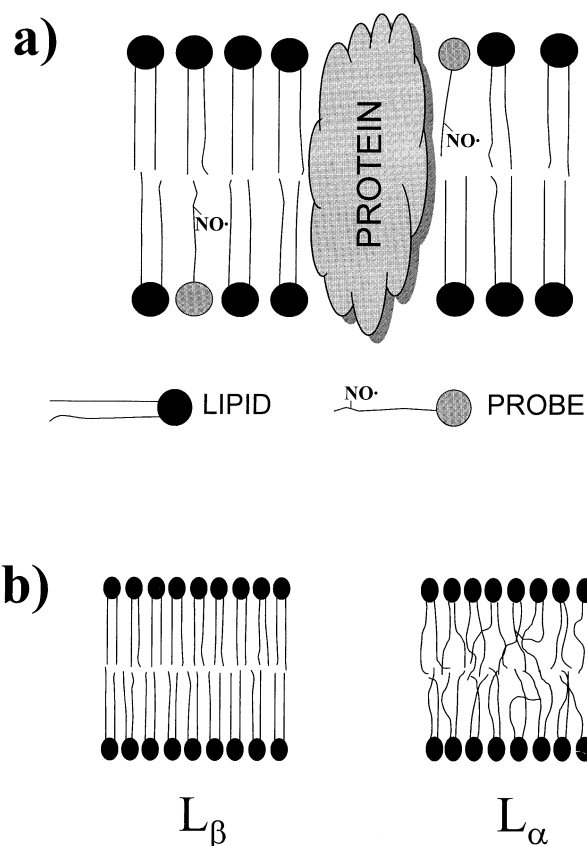


Fig. 7. (a) Sketch of the membrane structure. (b) Schematic representation of the L_β gel and liquid crystal L_α phases.

characterised by a progressive release of the lipid tail to rotate, bend and change the *trans-gauche* conformation of the carbons [23,24]. The phase transition from the L_β phase to the L_α phase has been reported in other thylakoid membranes to occur in a region between 250 K and 300 K, but always spanning nearly 40° [24,25]. The existence of some gradient of order along the hydrophobic chain in the thylakoid membranes is also remarkable [21].

The spin probes contain the paramagnetic (NO^\bullet) group bound to the 5th and 16th carbon atom, respectively, of the stearic acid molecule (Fig. 1). Its position in the stearic chain determines the depth of NO^\bullet location in the thylakoid membrane and the portion of membrane surrounding the paramagnetic group [21]. Therefore, the NO^\bullet group in the 5- and 16-*n*-SASL will be located near the polar head groups of the lipid bilayer and at the inner hydrophobic region of the membrane, respectively. As a consequence of some order gradient along the hydro-

phobic chains, different averaging stages are expected for the EPR spectra of 5- and 16-*n*-SASL probes, the latter being more averaged.

To understand the EPR spectra of the NO[•] probes it is also necessary to take into account that there are two types of sites for the probe in the inner hydrophobic region: generic sites in the bulk lipid and sites near the protein, with exchange processes within both sites [20,26]. These two sites differ in their mobility; the probe in bulk sites is more mobile than that bound to the protein due to the mutual interaction through their hydrophobic segments. Many studies (see [17,19,20,26,27]) have focused on lipid–protein interaction. In general, they have provided information about: (i) the stoichiometry of the lipid–protein association, (ii) the specificity of such an association, (iii) the conformational order in the lipid–protein interface and (iv) the fatty acid exchange between the general position and the position bound to the protein. Temperature dependence studies give dynamic information on thylakoid membranes; however, the thermal evolution of SASL probes below 260–273 K has not usually been measured [11,16].

At temperatures lower than 250 K we only detected the axial NO[•] signal with both 5-*n*-SASL and 16-*n*-SASL probes. At these temperatures, the membrane is in the ordered L_β gel phase and the spectra correspond to the ‘static’ situation. When the temperature increases two signals are observed in the spectra of the 16-*n*-SASL probe whereas only one seems to be present in the case of the 5-*n*-SASL probe. This fact can be understood taking into account the specificity of the interaction with the protein [15], and considering the penetration into the membrane of the paramagnetic entity due to the difference in its position in the aliphatic chain. The 5-*n*-SASL probe is affected by the outermost part of the membrane, which is the most ordered. Therefore, the presence of only one EPR signal in the spectrum could apparently be due either to the fact that the probe does not interact with the protein or that in both bulk sites and sites near the protein the constraints on the motion of the NO[•] probe close to the polar head groups are similar. The observed thermal evolution (see Figs. 2 and 3) corresponds to a slow motion situation and can be associated with the broad transition to the less ordered liquid-crystalline L_α phase. The strong coincidence of the ther-

mal behaviour of the 5-*n*-SASL probe in STR7 and WT membranes indicates that the order in the outermost part of the membrane is the same in the mutant as in the WT membrane. The interaction of the hydrophilic lipid heads with the water medium can also explain that.

The high temperature behaviour of the 16-*n*-SASL probe is richer. In this case two signals are observed. One corresponds to isotropic averaging in the fast motion limit, *isotropic* signal, and the other to an axial entity in the slow motion regime, *axial* signal. The first can be associated with probes in bulk sites whereas the *axial* one is assigned to probes interacting with the proteins. Considering that the 16-*n*-SASL probe is influenced by the inner part of the membrane, the thermal evolution of the isotropic signal monitors the behaviour of the aliphatic tails tumbling.

We will now focus on the differences found in the thermal behaviour depicted in Fig. 5. As we pointed out in Section 3, the aspects of the spectra from the STR7 mutant membrane are similar to those from the WT at about 5–10 K lower temperature. Changes in the aspect of the spectrum could be, in principle, associated with a modification of the relative population between the bulk and protein bound sites, to a different fluidity of the STR7 mutant and the WT membranes or to a different motion behaviour of the probes in the two membranes [11,16]. As we have reported previously [10], there is a small difference in the total lipid to protein ratio in the STR7 mutant membrane compared with that in the WT one. Anyhow, the mutant membrane has a lower protein content; thus the differences of the corresponding EPR spectra at a given temperature could never be explained by a decrease in the protein bound probe proportion. The correlation time for the isotropic motion measured at temperatures above 290 K (see Fig. 6) clearly shows that there is a lag of 5–10 K between the thermal evolution in the mutant as compared with the WT membrane. Although we have no quantitative data on the motion of the *axial* signal, the experimental results in Fig. 5 indicate the existence of a parallel behaviour of both membranes, with a lower fluidity of the STR7 mutant as compared with the WT thylakoid membrane.

The results reported here are consistent with the differences found in the chloroplastic lipids DGDG,

MGDG and PG, mainly at the C16:0, C16:1 and C18:3 levels. The thylakoid membrane of STR7 accumulates a high content of C16:0 and reduced levels of C16:1 and C18:3 fatty acids, as compared to WT [10]. The C18:3 is the most abundant trienoic fatty acid in the bulk lipids, conferring a high unsaturation degree and consequently appropriate fluidity properties to the thylakoid membrane in plants [1,4,28,29]. More saturated fatty acids (i.e. C16:1) have been considered as specific lipids involved in interaction with proteins [28,30–34]. Thus, changes in both kinds of lipid would explain the lower fluidity observed in the STR7 thylakoid membrane.

According to that, our results seem to indicate that the change in the unsaturation level of fatty acids in STR7 is the main factor that influences the motion of probes in the inner hydrophobic region of its thylakoid membrane. This fact is in agreement with the model of organisation of lipids in thylakoid membranes [28].

On the other hand, we have reported previously that the STR7 mutant presents an increased tolerance to high temperatures [10]. In that sense, further research is necessary to establish whether lipid content, fatty acid composition and changes in the thylakoid membrane fluidity are related with such thermal stress behaviour.

Acknowledgements

The authors are grateful to Maria V. Ramiro for skilful technical assistance. M.A. and I.G.-R. were recipients of a contract and a fellowship, respectively, from the Ministerio de Educación y Cultura of Spain. This work was supported by the Dirección General de Investigación Científica y Técnica (Grant PB98-1632) and by the Diputación General de Aragón (Project P17/98).

References

- [1] P.-A. Siegenthaler, A. Trémolières, in: P.-A. Siegenthaler, N. Murata (Eds.), *Lipids in Photosynthesis; Structure, Function and Genetics*, Vol. 6, Kluwer Academic Publishers, Dordrecht, 1998, pp. 145–173.
- [2] P.-O. Arvidsson, C. Sundby, *Aust. J. Plant Physiol.* 26 (1999) 687–694.
- [3] J.M. Anderson, *Aust. J. Plant Physiol.* 26 (1999) 625–639.
- [4] N. Murata, P.-A. Siegenthaler, in: P.-A. Siegenthaler, N. Murata (Eds.), *Lipids in Photosynthesis; Structure, Function and Genetics*, Vol. 6, Kluwer Academic Publishers, Dordrecht, 1998, pp. 1–20.
- [5] J.L. Harwood, in: P.-A. Siegenthaler, N. Murata (Eds.), *Lipids in Photosynthesis; Structure, Function and Genetics*, Vol. 6, Kluwer Academic Publishers, Dordrecht, 1998, pp. 287–302.
- [6] I. Nishida, N. Murata, *Annu. Rev. Plant Physiol. Plant Mol. Biol.* 47 (1996) 541–568.
- [7] G.R. Orr, J.K. Raison, *Plant Physiol.* 84 (1987) 88–92.
- [8] Y. Tasaka, Z. Gombos, Y. Nishiyama, P. Mohanty, T. Ohba, K. Ohki, N. Murata, *EMBO J.* 23 (1996) 6416–6425.
- [9] M. Alfonso, J.J. Pueyo, K. Gaddour, A.-L. Etienne, D. Kirilovsky, R. Picorel, *Plant Physiol.* 112 (1996) 1499–1508.
- [10] M. Alfonso, I. Yruela, S. Almárcegui, E. Torrado, M.A. Pérez, R. Picorel, *Planta* 212 (2001) 573–582.
- [11] G. Li, P.F. Knowles, D.J. Murphy, D. Marsh, *J. Biol. Chem.* 265 (1990) 16867–16872.
- [12] R.C. Ford, J. Barber, *Planta* 158 (1983) 35–41.
- [13] G. Li, L.I. Horváth, P.F. Knowles, D.J. Murphy, D. Marsh, *Biochim. Biophys. Acta* 987 (1989) 187–192.
- [14] G. Li, P.F. Knowles, D.J. Murphy, I. Nishida, M. Derek, *Biochim. Biophys. Acta* 28 (1989) 7446–7452.
- [15] A. Ivancich, L.I. Horváth, M. Droppa, G. Horváth, T. Farkas, *Biochim. Biophys. Acta* 1196 (1994) 51–56.
- [16] M.F. Quartacci, C. Pinzino, C.L.M. Sgherri, F.D. Vecchia, F. Navari-Izzo, *Physiol. Plant.* 108 (2000) 87–93.
- [17] D. Marsh, in: Watt, Du Pont (Eds.), *Progress in Protein-Lipid Interactions*, Elsevier Science Publishers, Amsterdam, 1985, pp. 143–172.
- [18] D. Marsh, *Biosci. Rep.* 19 (1999) 253–259.
- [19] D. Marsh, L.I. Horváth, in: A.J. Hoff (Ed.), *Advanced EPR. Application in Biology and Biochemistry*, Elsevier Science Publishers, Amsterdam, 1989, pp. 707–812.
- [20] D. Marsh, L.I. Horváth, *Biochim. Biophys. Acta* 1376 (1998) 267–296.
- [21] A. Ligeza, A.N. Tikhonov, J.S. Hyde, W.K. Subczynski, *Biochim. Biophys. Acta* 1365 (1998) 453–463.
- [22] A. Carrington, A.D. McLachlan, in: *Introduction to Magnetic Resonance*, Chapman and Hall, London, 1979, pp. 197–200.
- [23] C.E. Fairhurst, S. Fuller, J. Gray, M.C. Holmes, G.J.T. Tiddy, in: D. Demus, J. Goodby, G.W. Gray, H.W. Spiess (Eds.), *Handbook of Liquid Crystals*, Vol. 3, Wiley-VCH, Weinheim, 1998, pp. 354 and ff.
- [24] W.P. Williams, B.A. Cunningham, D.H. Wolfe, G.E. Derbyshire, G.R. Mant, W. Bras, *Biochim. Biophys. Acta* 1284 (1996) 86–96.
- [25] D.A. Mannock, A.P.R. Brain, W.P. Williams, *Biochim. Biophys. Acta* 821 (1985) 153–164.

- [26] D. Mihailescu, L.I. Horváth, *Eur. Biophys. J.* 28 (1999) 216–221.
- [27] D. Marsh, *Biochemistry* B426 (1982) 1–44.
- [28] S. Duchêne, P.-A. Siegenthaler, *Lipids* 35 (2000) 739–744.
- [29] P.-A. Siegenthaler, in: P.-A. Siegenthaler, N. Murata (Eds.), *Lipids in Photosynthesis; Structure, Function and Genetics*, Vol. 6, Kluwer Academic Publishers, Dordrecht, 1998, pp. 119–144.
- [30] B.R. Jordan, W.S. Chow, A.J. Baker, *Biochim. Biophys. Acta* 725 (1983) 77–86.
- [31] P.-A. Siegenthaler, J. Smutny, A. Rawler, *Biochim. Biophys. Acta* 891 (1987) 85–93.
- [32] O. Kruse, G.H. Schmid, *Z. Naturforsch.* 50c (1995) 380–390.
- [33] O. Kruse, B. Hankamer, C. Konczak, C. Gerle, E. Morris, A. Radunz, G.H. Schmid, J. Barber, *J. Biol. Chem.* 275 (2000) 6509–6514.
- [34] M. Hagio, Z. Gombos, Z. Várkonyi, K. Massamoto, N. Sato, M. Tsuzuki, H. Wada, *Plant Physiol.* 124 (2000) 795–804.